Multi-stimuli responsive heterotypic hydrogels based on nucleolipids show selective dye adsorption

Ashok Nuthanakanti and Seergazhi G. Srivatsan*

Department of Chemistry, Indian Institute of Science Education and Research, Pune
Dr. Homi Bhabha Road, Pashan, Pune 411008, India

Electronic Supplementary Information (ESI)

1. Materials: Ribothymidine, 2,2-dimethoxypropane (DMP), dodecanoic acid, palmatic acid, eosine Y, methyl orange, methylene blue, rhodamine 6G, tetrabutylammonium chloride, 15-crown-5, p-toluenesulfonic acid and camphorsulfonic acid were purchased from Sigma-Aldrich. EDC (1-(3-dimethyl aminopropyl)-3-ethyl carbodiimide hydrochloride), 4-dimethylaminopyridine were obtained from Avera Synthesis Pvt. Limited and uridine from Molychem. Myristic acid was procured from Fluka. Silicon wafers (N-type without dopant) were purchased from Sigma-Aldrich.

2. Instrumentation: NMR spectra were recorded on 400 MHz Jeol ECS-400 spectrometer and Bruker 500 MHz spectrometer. Absorption spectra were recorded on a Shimadzu UV-2600 spectrophotometer in a micro fluorescence cuvette (Hellma, path length 1.0 cm). The morphology of gels was analyzed using Zeiss Ultra Plus field-emission scanning electron microscope (FESEM). Powder X-ray diffraction (PXRD) spectra were obtained at room temperature using Bruker D8 Advance diffractometer (Cu Kα radiation, λ = 1.5406 Å). Single crystal X-ray data for structure determination were collected from Bruker APEX II DUO diffractometer using MoKα (λ= 0.71073 Å) graphite monochromated radiation. MCR-302 (Anton-Paar) rheometer was used for Rheological studies.

3. Characterization data for nucleolipids 3a–3c and 4a–4c

3a: Colourless, 27 % yield over two steps, TLC (CH_2Cl_2:MeOH = 95:5 with few drops of Et_3N); R_f = 0.28; ^{1}H NMR (400 MHz, DMSO-d_6): δ (ppm) 11.35 (s, 1H), 7.43 (d, *J* = 1.2 Hz, 1H), 5.77 (d, *J* = 5.2 Hz, 1H), 5.42 (d, *J* = 5.6 Hz, 1H), 5.25 (d, *J* = 5.6 Hz. 1H), 4.26–4.18 (m, 2 H), 4.09–4.06 (m, 1H), 3.98–3.92 (m, 1H), 2.33 (t, *J* = 7.2 Hz, 2H), 1.79 (d, *J* = 1.2 Hz, 3H), 1.55–1.48 (m, 2 H), 1.27–1.23 (m, 16H), 0.85 (t, *J* = 6.8 Hz, 3H); ^{13}C NMR (100 MHz, DMSO-d_6): δ (ppm) 172.7, 163.6, 150.7, 136.2, 109.7, 88.2, 81.0, 72.5, 69.8, 63.6, 33.4, 31.3, 29.0, 28.9, 28.7, 28.6, 28.4, 24.4, 22.1, 14.0, 12.1; HRMS: m/z Calcd. for $C_{22}H_{37}N_2O_7[M+H]^+$ = 441.2601, found = 441.2606.

3b: Colourless, 29 % yield over two steps, TLC (CH_2Cl_2:MeOH = 95:5 with few drops of Et_3N); R_f = 0.43; ^{1}H NMR (400 MHz, DMSO-d_6): δ (ppm) 11.35 (s, 1H), 7.43 (d, *J* = 1.2 Hz, 1H), 5.77 (d, *J* = 5.2 Hz, 1H), 5.42 (d, *J* = 5.6 Hz, 1H), 5.25 (d, *J* = 5.2 Hz. 1H), 4.26–4.17 (m, 2 H), 4.09–4.06 (m, 1H), 3.98–3.92 (m, 2H), 2.33 (t, *J* = 7.2 Hz, 2H), 1.79 (d, *J* = 0.8 Hz, 3H), 1.55–1.48 (m, 2 H), 1.27–1.23 (m, 20H), 0.85 (t, *J* = 6.8 Hz, 3H); ^{13}C NMR (100 MHz, DMSO-d_6): δ (ppm) 172.7, 163.6, 150.7, 136.7, 109.7, 88.2, 81.0, 72.5, 69.8, 63.6, 33.4, 31.3, 29.0, 29.0, 28.9, 28.8, 28.7, 28.6, 28.4, 24.4, 22.1, 13.9, 12.1; HRMS: m/z Calcd. for $C_{24}H_{41}N_2O_7[M+H]^+$ = 469.2914, found = 469.2917.

3c: Colourless, 30 % yield over two steps, TLC (CH_2Cl_2:MeOH = 95:5 with few drops of Et_3N); R_f = 0.42; ^{1}H NMR (400 MHz, DMSO-d_6): δ (ppm) 11.35 (s, 1H), 7.43 (d, *J* = 1.2 Hz, 1H), 5.77 (d, *J* = 5.2 Hz, 1H), 5.42 (d, *J* = 5.6 Hz, 1H), 5.25 (d, *J* = 5.2 Hz. 1H), 4.26–4.17 (m, 2 H), 4.09–4.05 (m, 1H), 3.98–3.92 (m, 2H), 2.33 (t, *J* = 7.2 Hz, 2H), 1.79 (d, *J* = 0.8 Hz, 3H), 1.55–1.48 (m, 2 H), 1.27–1.23 (m, 24H), 0.85 (t, *J* = 6.8 Hz, 3H); ^{13}C NMR (100 MHz, DMSO-d_6): δ (ppm) 172.7, 163.6, 150.7, 136.1, 109.7, 88.2, 81.0, 72.5, 69.8, 63.6, 33.4, 31.3, 29.0, 29.0, 29.0, 29.0, 28.9, 28.7, 28.6, 28.4, 24.4, 22.1, 13.9, 12.1; HRMS: m/z Calcd. for $C_{26}H_{45}N_2O_7[M+H]^+$ = 497.3227, found = 497.3228.

4a: Colourless, 22 % yield over two steps, TLC (CH_2Cl_2:MeOH = 95:5 with few drops of Et_3N); R_f = 0.39; ^{1}H NMR (400 MHz, DMSO-d_6): δ (ppm) 11.36 (s, 1H), 7.61 (d, J = 8.0 Hz, 1H), 5.74 (d, J = 5.2 Hz, 1H), 5.64 (dd, J_1 = 8.0 Hz, J_2 = 1.2 Hz, 1H), 5.47 (d, J = 5.2 Hz. 1H), 5.27 (d, J = 5.6 Hz, 1H),4.24 (dd, J_1 = 12.0 Hz, J_2 = 3.2 Hz, 1H), 4.17 (dd, J_1 = 12.4 Hz, J_2 = 5.6 Hz, 1H), 4.09–4.05 (m, 1H), 4.00–3.96 (m, 1H), 3.94–3.90 (m, 1H), 2.33 (t, J = 7.4 Hz, 2H), 1.54–1.47 (m, 2H), 1.27–1.23 (m, 16H), 0.85 (t, J = 6.8 Hz, 3H); ^{13}C NMR (100 MHz, DMSO-d_6): δ (ppm) 172.7, 163.0, 150.6, 140.7, 101.9, 88.7, 81.1, 72.7, 69.7, 63.6, 33.3, 31.3, 29.0, 28.9, 28.7, 28.7, 28.4, 24.4, 22.1, 14.0; HRMS: m/z Calcd. for $C_{21}H_{35}N_2O_7[M+H]^+$ = 427.2444, found = 427.2453.

4b: Colourless, 20 % yield over two steps, TLC (CH_2Cl_2:MeOH = 95:5 with few drops of Et_3N); R_f = 0.37; ^{1}H NMR (400 MHz, DMSO-d_6): δ (ppm) 11.36 (s, 1H), 7.62 (d, J = 8.4 Hz, 1H), 5.74 (d, J = 4.8 Hz, 1H), 5.64 (d, J = 8.0 Hz, 1H), 5.47 (d, J = 5.6 Hz. 1H), 5.27 (d, J = 5.6 Hz, 1H),4.24 (dd, J_1 = 12.0 Hz, J_2 = 3.6 Hz, 1H), 4.17 (dd, J_1 = 12.0 Hz, J_2 = 5.6 Hz, 1H), 4.08–4.05 (m, 1H), 4.00–3.96 (m, 1H), 3.94–3.90 (m, 1H), 2.32 (t, J = 7.4 Hz, 2H), 1.53–1.48 (m, 2H), 1.27–1.23 (m, 20H), 0.85 (t, J = 6.8 Hz, 3H); ^{13}C NMR (100 MHz, DMSO-d_6): δ (ppm) 172.7, 163.0, 150.6, 140.7, 101.9, 88.7, 81.1, 72.7, 69.7, 63.6, 33.3, 31.3, 29.0, 29.0, 29.0, 28.9, 28.7, 28.7, 28.4, 24.4, 22.1, 14.0; HRMS: m/z Calcd. for $C_{23}H_{39}N_2O_7[M+H]^+$ = 455.2757, found = 455.2768.

4c: Colourless, 21 % yield over two steps, TLC (CH_2Cl_2:MeOH = 95:5 with few drops of Et_3N); R_f = 0.36; ^{1}H NMR (400 MHz, DMSO-d_6): δ (ppm) 11.36 (s, 1H), 7.62 (d, J = 8.0 Hz, 1H), 5.74 (d, J = 5.2 Hz, 1H), 5.64 (dd, J_1 = 8.0 Hz, J_2 = 2.0 Hz, 1H), 5.46 (d, J = 5.6 Hz. 1H), 5.27 (d, J = 5.6 Hz, 1H), 4.24 (dd, J_1 = 12.0 Hz, J_2 = 3.2 Hz, 1H), 4.17 (dd, J_1 = 12.0 Hz, J_2 = 5.6 Hz, 1H), 4.09–4.05 (m, 1H), 4.00–3.96 (m, 1H), 3.94–3.90 (m, 1H), 2.33 (t, J = 7.4 Hz, 2H), 1.55–1.48 (m, 2H), 1.27–1.23 (m, 24H), 0.85 (t, J = 6.8 Hz, 3H); ^{13}C NMR (100 MHz, DMSO-d_6): δ (ppm) 172.7, 163.0, 150.6, 140.7, 101.9, 88.7, 81.0, 72.7, 69.7, 63.6, 33.3, 31.3, 29.0, 29.0, 29.0, 28.9, 28.7, 28.7, 28.4, 24.4, 22.1, 13.9; HRMS: m/z Calcd. for $C_{25}H_{43}N_2O_7[M+H]^+$ = 483.3070, found = 483.3066.

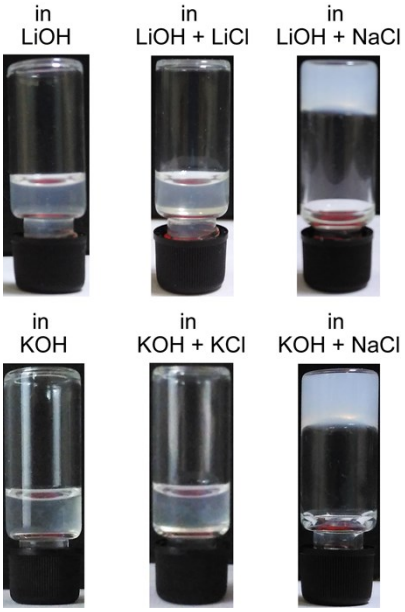

Fig. S1 Role of cations in the gelation process of nucleolipid **3b**. Addition of 0.05 M NaCl to an aqueous solution of nucleolipid **3b** containing either KOH or LiOH resulted in efficient sol-gel transition, which was not observed when LiCl or KCl was added.

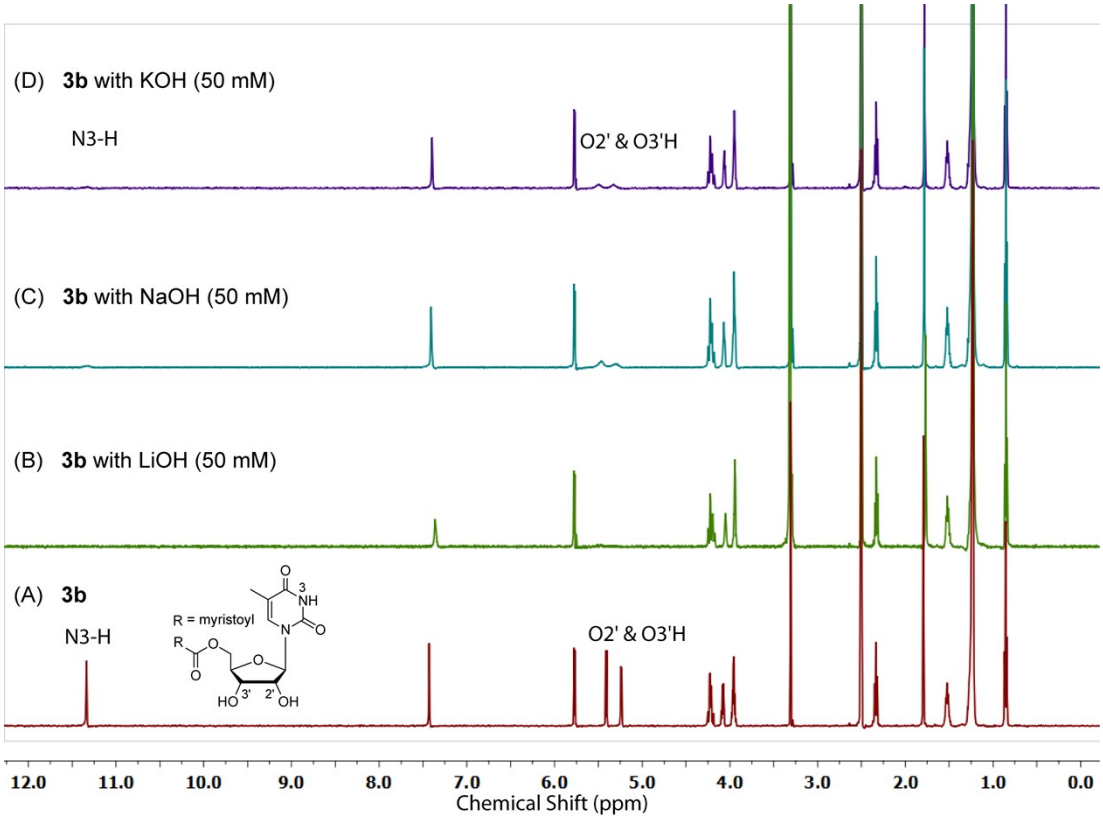

Fig. S2 ^{1}H NMR spectra of nucleolipid **3b** at CGC (0.3 w/v %) in DMSO-d_6, (A) compound **3b** alone, (B) **3b** with 50 mM LiOH, (C) **3b** with 50 mM NaOH and (D) **3b** with 50 mM KOH. Hydrogen bonding sites of **3b** N3-H, O2'H & O3'H protons are deprotonated upon addition of bases. Bases were added in solid form.

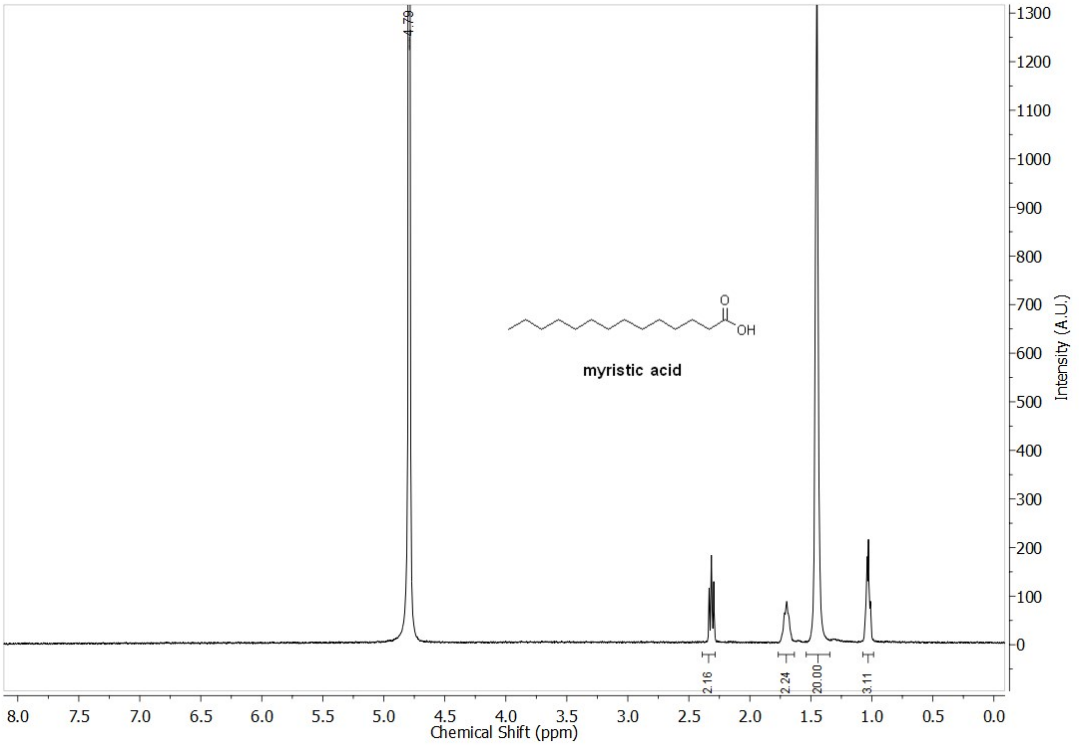

Fig. S3 ^{1}H NMR spectrum of hydrogel of myristic acid **5** (6.4 mM) with 0.05 M NaOH in D_2O. Spectrum was taken at 40 °C.

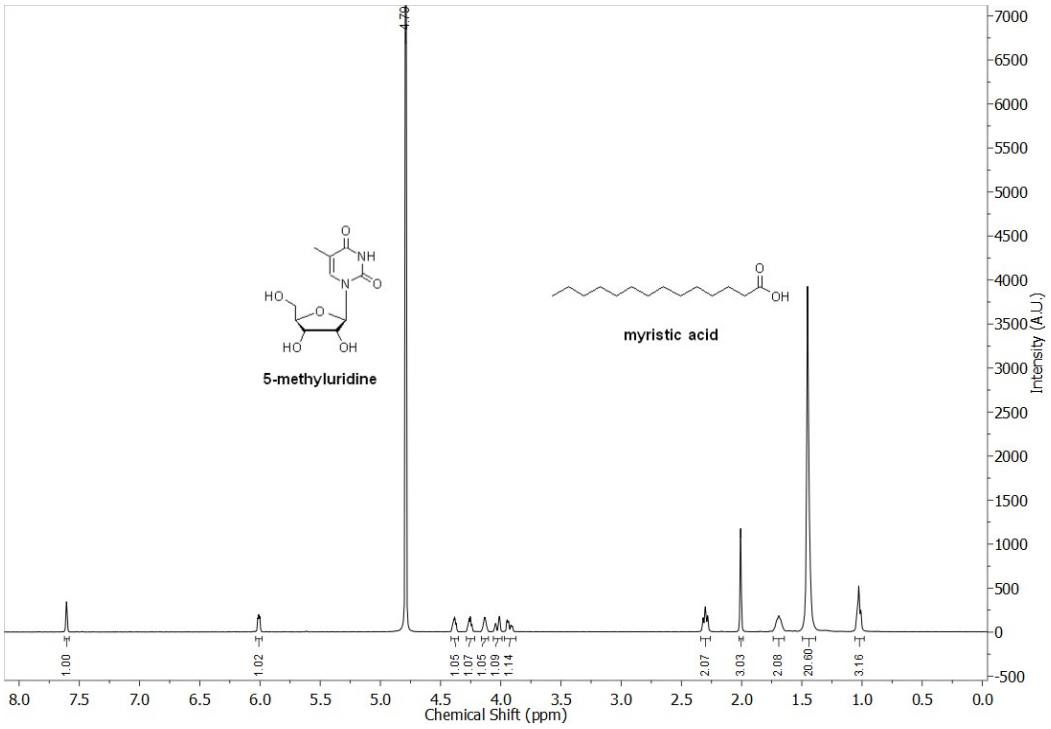

Fig. S4 ^{1}H NMR spectrum of hydrogel of ribothymidine and myristic acid combination (**5•1a**, 6.4 mM) with 0.05 M NaOH in D_2O at 40 °C. The molar ratio of ribothymidine:myristic acid is 1:1 by comparing the peak integration.

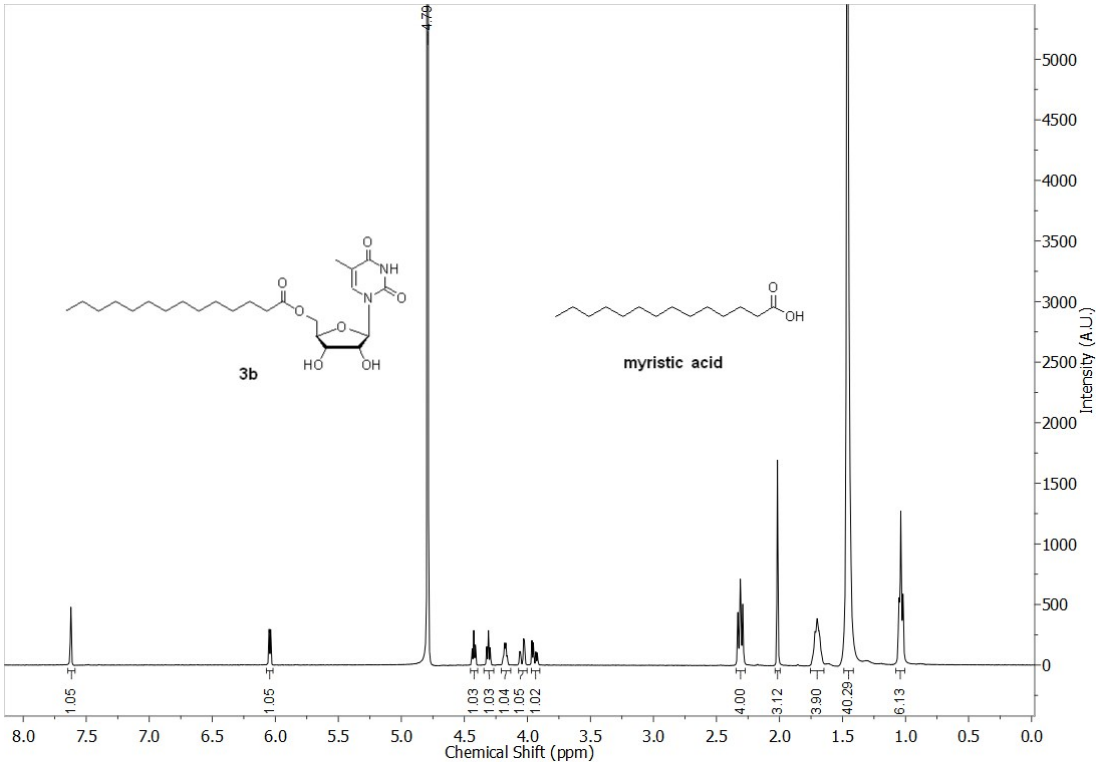

Fig. S5A ^{1}H NMR spectrum of heterotypic hydrogel formed using **3b** (6.4 mM) with 0.05 M NaOH in D_2O at 40 °C after 12 h. The molar ratio of nucleolipid **3b**:myristic acid is 1:1 as obtained by comparing the peak integration.

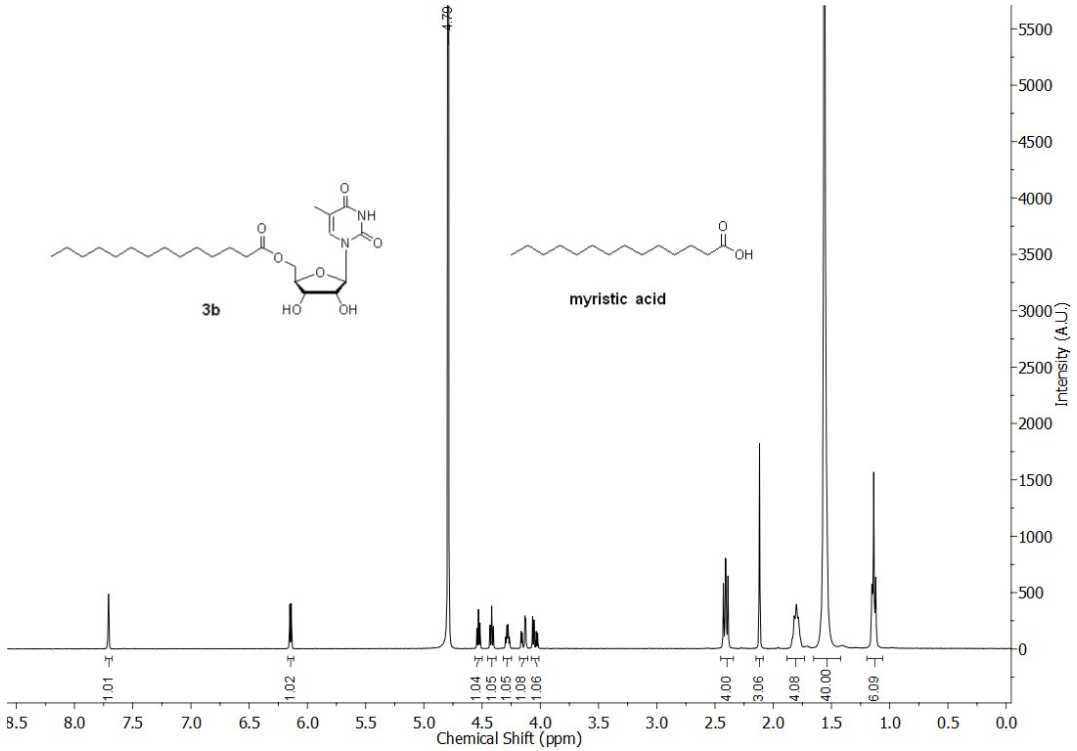

Fig. S5B ^{1}H NMR spectrum of heterotypic hydrogel formed using **3b** (6.4 mM) with 0.05 M NaOH in D_2O at 40 °C. NMR spectrum was taken after one week. The molar ratio of nucleolipid **3b**:myristic acid is 1:1 as obtained by comparing the peak integration.

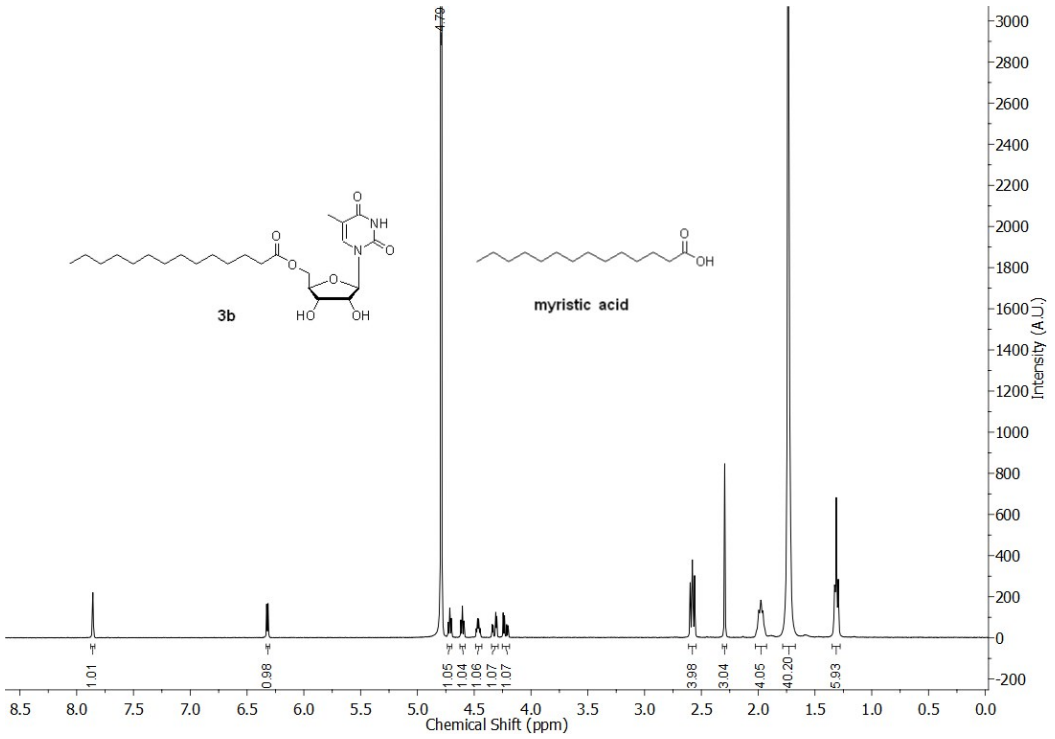

Fig. S5C ^{1}H NMR spectrum of the sol form of the heterotypic hydrogel formed using **3b** (6.4 mM) with 0.05 M NaOH in D_2O at 65 °C. The molar ratio of nucleolipid **3b**:myristic acid is 1:1 as obtained by comparing the peak integration.

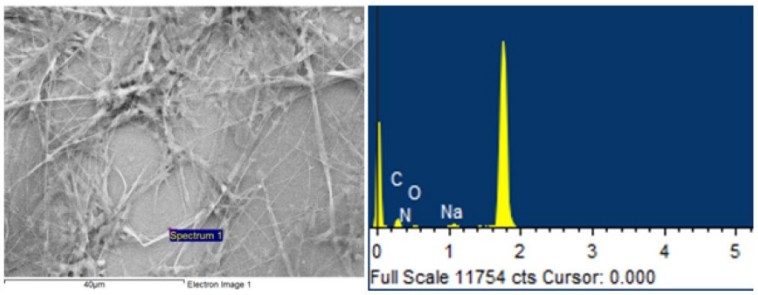

Element	Weight%	Atomic%
C K	57.34	65.12
N K	4.05	3.94
O K	30.95	26.39
Na K	7.66	4.55
Totals	100.00	

Fig. S6 EDAX analysis of hydrogel formed using **3b** in the presence of 0.05 M NaOH suggests that the gel network is made of 1:1 ratio of nucleolipid **3b** and myristate salt.
Calculated elemental composition of nucleolipid **3b** and myristic acid sodium salts is ($C_{38}H_{64}N_2Na_3O_9$) C: 59.9, H: 8.47, N: 3.68, O: 18.9 and Na: 9.05, which is nearly the weight percentage of fiber composition. We see slightly higher percentage of oxygen, which could be due to water molecules trapped in the fiber network of the hydrogel.

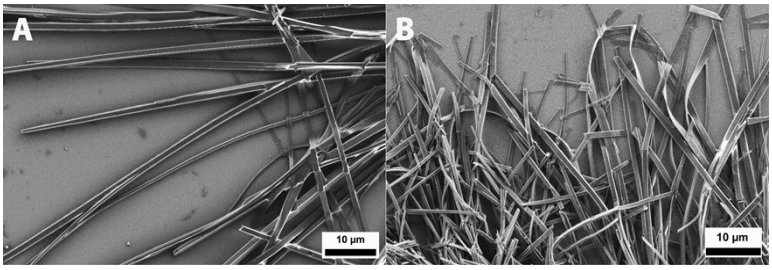

Fig. S7 (**A** and **B**) FESEM images of xerogels of **3b** and **3c** formed in chloroform, respectively.

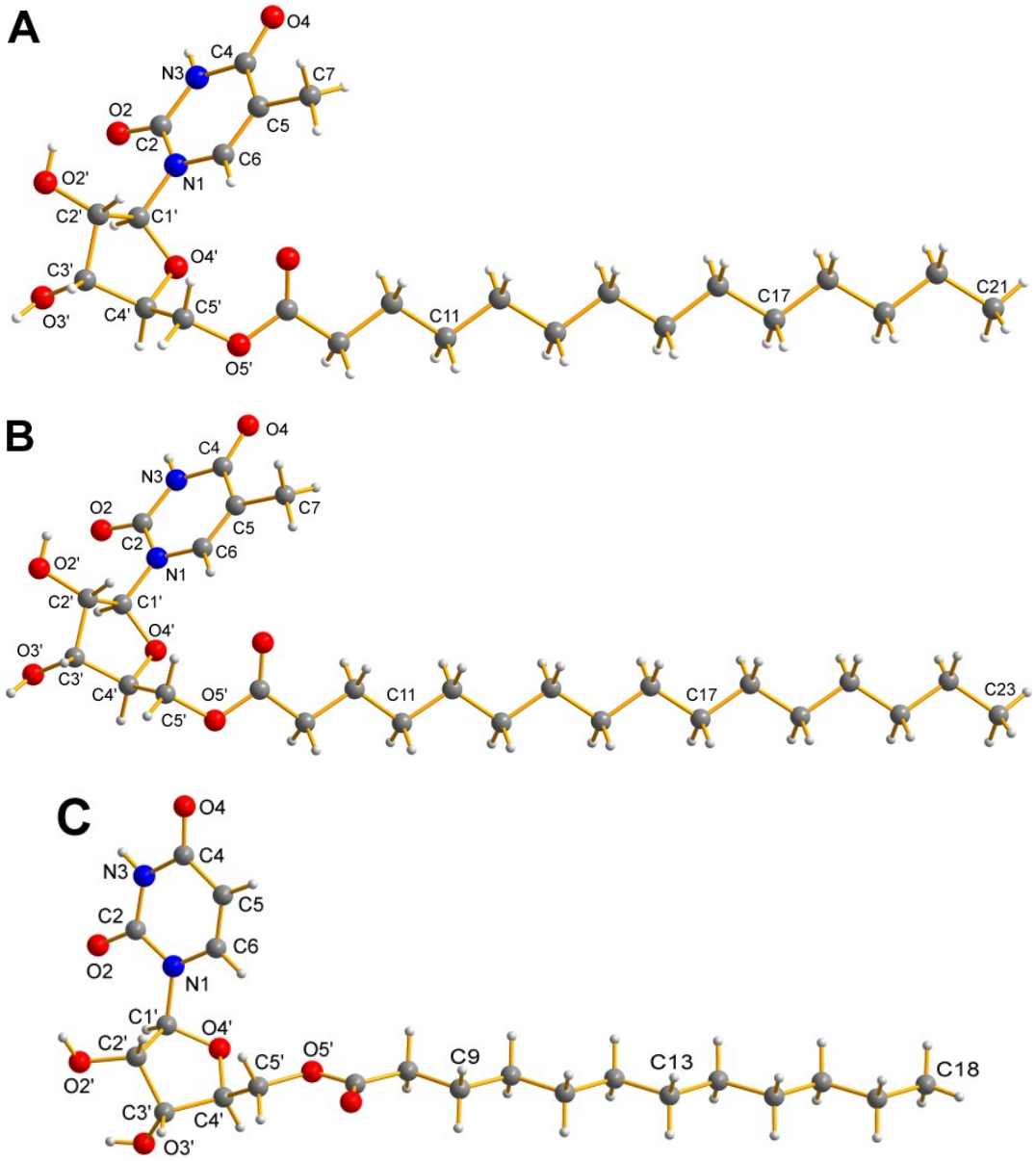

Fig. S8 A–C: X-ray crystal structures of nucleolipids **3b**, **3c** and **4a** showing one molecule in the unit cell. Nucleobase adopts an *anti* conformation relative to the sugar ring with C2′-endo puckered sugar. Atoms are coded as follows: off white, hydrogen; dark gray, carbon; blue, nitrogen; red, oxygen.

Table S1. Crystallographic data for nucleolipid **(3b)**

Compound identity	**3b**
Empirical formula	$C_{24}H_{40}N_2O_7$
Formula weight	468.58
Temperature	296(2) K
Wavelength	0.71073 Å
Crystal system	Monoclinic
Space group	P 21
Unit cell dimensions	a = 9.0437(11) α = 90 b = 5.1046(7) β = 93.688(3) c = 26.820(3) γ = 90
Volume	1235.6(3) $Å^3$
Z	2
Density (calculated)	1.259 Mg/cm^3
Absorption coefficient (μ)	0.092 mm^{-1}
F(000)	508
Crystal size	0.65 X 0.35 X 0.24 mm^3
Theta range for data collection	0.76 to 31.07
Index ranges	-12<=h<=11, -6<=k<=7, -35<=l<=38
Reflections collected	20006
Independent reflections	5462 [R(int) = 0.0448]
Completeness to theta = 31.07	96.0 %
Absorption correction	MULTI-SCAN
Max. and min. Transmission	0.978 and 0.962
Refinement method	Full-matrix least-squares on F^2
Data / restraints / parameters	5462 / 1 / 302
Goodness-of-fit on F^2	1.071
Final R indices [I>2sigma(I)]	R1 = 0.0397, wR2 = 0.0984
R indices (all data)	R1 = 0.0494, wR2 = 0.1094
Largest diff. Peak and hole	0.302 and -0.332 $e.Å^{-3}$
CCDC	1554880

Table S2. Crystallographic data for nucleolipid **(3c)**

Compound identity	**3c**
Empirical formula	$C_{26}\ H_{44}\ N_2\ O_7$
Formula weight	496.63
Temperature	296(2) K
Wavelength	0.71073 Å
Crystal system	Monoclinic
Space group	P 21
Unit cell dimensions	a = 9.0191(9) α = 90 b = 5.0832(6) β = 96.335(3) c = 28.934(3) γ = 90
Volume	1318.4(2) $Å^3$
Z	2
Density (calculated)	1.251 Mg/cm^3
Absorption coefficient (μ)	0.090 mm^{-1}
F(000)	540
Crystal size	0.38 X 0.25 X 0.03 mm^3
Theta range for data collection	2.27 to 27.26
Index ranges	-11<=h<=11, -6<=k<=6, -37<=l<=37
Reflections collected	49660
Independent reflections	6102 [R(int) = 0.1163]
Completeness to theta = 27.56	99.7 %
Absorption correction	MULTI-SCAN
Max. and min. Transmission	0.997 and 0.973
Refinement method	Full-matrix least-squares on F^2
Data / restraints / parameters	6102 / 1 / 320
Goodness-of-fit on F^2	1.043
Final R indices [I>2sigma(I)]	R1 = 0.0564, wR2 = 0.1109
R indices (all data)	R1 = 0.0943, wR2 = 0.1234
Largest diff. Peak and hole	0.270 and -0.302 $e.Å^{-3}$
CCDC	1554881

Table S3. Crystallographic data for nucleolipid **(4a)**

Compound identity	**4a**
Empirical formula	$C_{21}H_{34}N_2O_7$
Formula weight	426.50
Temperature	296(2) K
Wavelength	0.71073 Å
Crystal system	Monoclinic
Space group	P 21
Unit cell dimensions	a = 8.243(5) α = 90 b = 4.862(3) β = 93.566(13) c = 26.967(14) γ = 90
Volume	1080.7(10) $Å^3$
Z	2
Density (calculated)	1.311 Mg/cm^3
Absorption coefficient (μ)	0.098 mm^{-1}
F(000)	460
Crystal size	0.72 X 0.28 X 0.12 mm^3
Theta range for data collection	0.75 to 25.34
Index ranges	-9<=h<=9, -5<=k<=5, -32<=l<=32
Reflections collected	16280
Independent reflections	3869 [R(int) = 0.0625]
Completeness to theta = 25.34	99.8 %
Absorption correction	MULTI-SCAN
Max. and min. Transmission	0.988 and 0.968
Refinement method	Full-matrix least-squares on F^2
Data / restraints / parameters	3869/ 1 / 275
Goodness-of-fit on F^2	0.775
Final R indices [I>2sigma(I)]	R1 = 0.0418, wR2 = 0.1027
R indices (all data)	R1 = 0.0550, wR2 = 0.1210
Largest diff. Peak and hole	0.532 and -0.417 $e.Å^{-3}$
CCDC	1554882

Table S4. H-bonding distances and angles, torsional angles measured from the crystal structure of ribothymidine and uridine nucleolipids **3b**, **3c** and **4a**.

Nucleolipid	Hydrogen bond	Distance (Å)	Angle (°)	Torsion angle (χ) (°)
3b	N3H---O2'	2.384(1)	115.1(1)	C2-N1-C1'-O4' 139.0(1)
	O2---HO2'	1.845(1)	170.1(1)	
	O2'H---O2	1.845(1)	170.1(1)	
	O2'---HN3	2.384(1)	115.1(1)	
	O2'---HO3'	1.937(1)	168.3(1)	
	O3'---HO2'	1.937(1)	168.3(1)	
	O8---HC6	2.349(1)	152.1(1)	
3c	N3H---O2'	2.378(2)	115.4(1)	C2-N1-C1'-O4' 139.3(2)
	O2---HO2'	1.840(2)	169.4(2)	
	O2'H---O2	1.840(2)	169.4(2)	
	O2'---HN3	2.378(2)	115.4(2)	
	O2'---HO3'	1.941(2)	163.9(1)	
	O3'---HO2'	1.941(2)	163.9(1)	
	O8---HC6	2.360(1)	151.6(2)	
4a	O4---HN3	1.972(2)	177.8(2)	C2-N1-C1'-O4' 144.6(2)
	O4---HO3'	1.980(2)	152.7(1)	
	N3H---O4	1.972(2)	177.8(2)	
	O2--- HO2'	1.914(2)	176.1(1)	
	O2'H---O2	1.914(2)	176.1(1)	
	O3'H---O4	1.980(2)	152.7(2)	

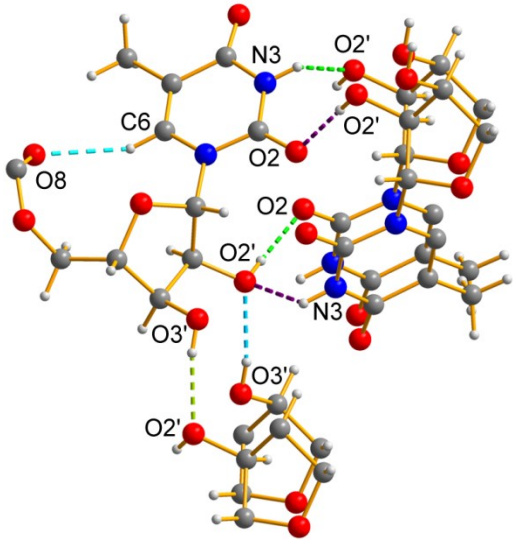

Fig. S9 X-ray crystal structure of **3c** showing a detailed view of the H-bonding interactions along the crystallographic b-axes, which is similar to **3b**.

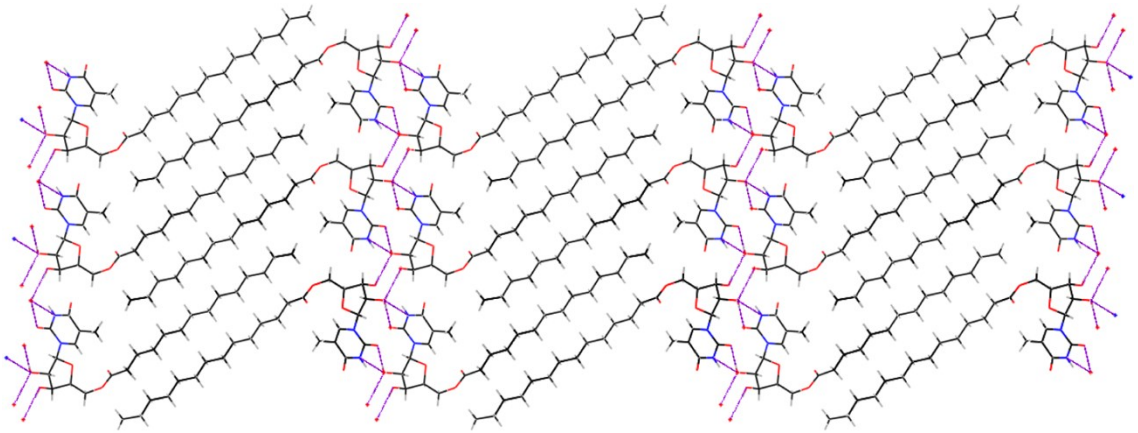

Fig. S10 Complete packing diagram of **3b** along the crystallographic b-axes.

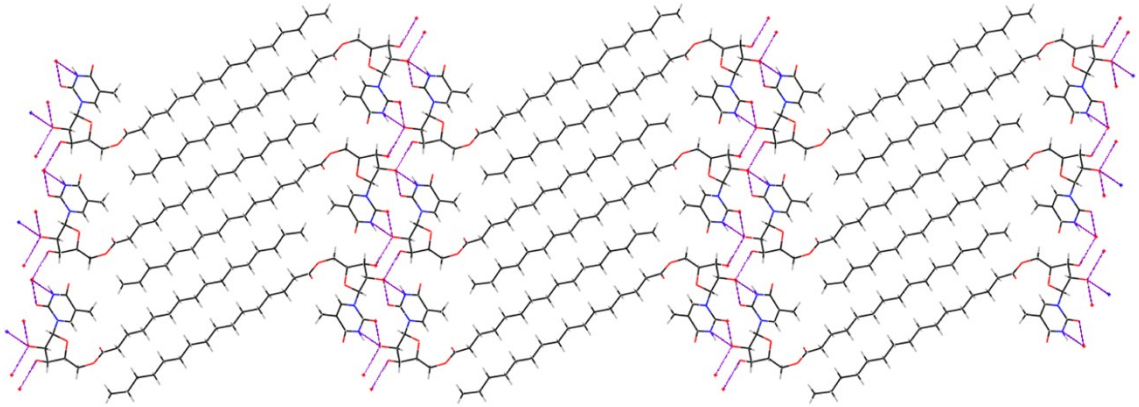

Fig. S11 Complete packing diagram of **3c** along the crystallographic b-axes.

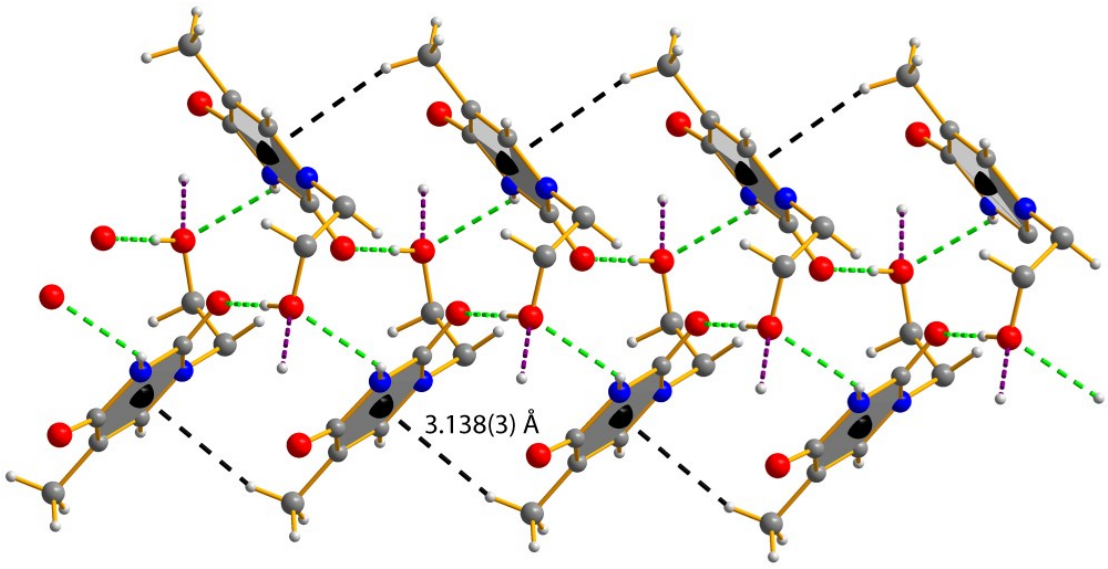

Fig. S12 X-ray crystal structure of nucleolipid **3b** showing CH-π stacking interaction between the C5-methyl hydrogen of ribothymidine group with adjacent thymine ring along the crystallographic b-axes. The CH-π stacking distance (3.138(3) Å) is shown in black dashed lines. H-bonding interactions are shown in green and violet dashed lines. Long chain acyl chains and ribose are not shown for sake of clarity. Atoms are coded as follows: off white, hydrogen; dark gray, carbon; blue, nitrogen; red, oxygen.

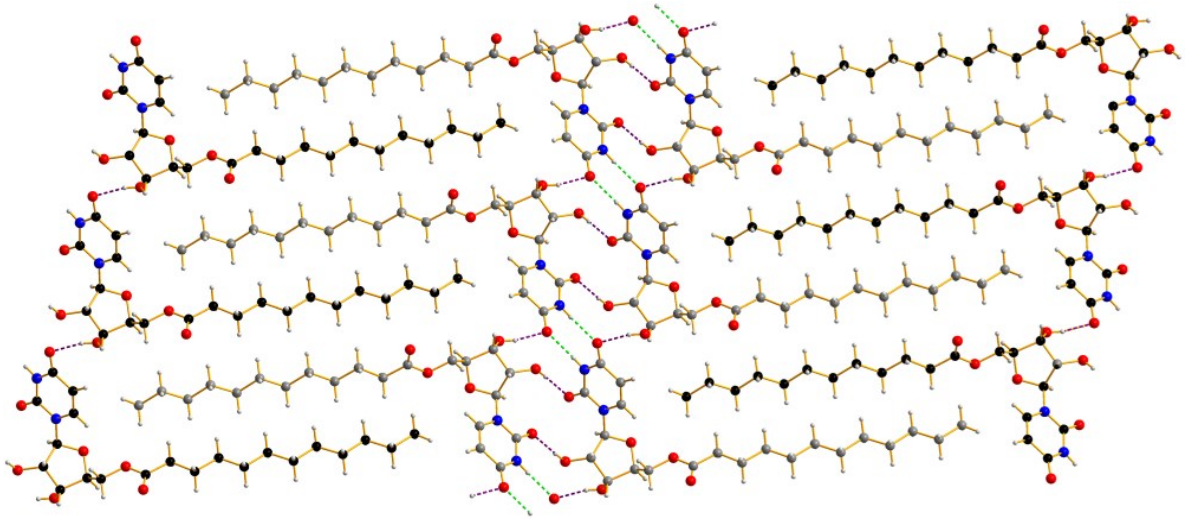

Fig. S13 X-ray crystal structure showing a complete view of the fully interdigitated alkyl chains of nucleolipid **4a** along the crystallographic b-axes. Here two 2D-sheets join together through strong interlayer hydrophobic interactions. For sake of clarity interdigitated alkyl chain carbons are indicated in black colour. Base recognition parts are shown in green dashed lines; other H-bonds are denoted in violet dashed lines. Atoms are coded as follows: off white, hydrogen; dark gray, carbon; blue, nitrogen; red, oxygen.

4. Powder X-ray diffraction (PXRD) analysis of nucleolipid gels: Hot solutions of **3b** in 50 mM NaOH, **3b** in benzene and **3c** in benzene at respective CGC were drop-casted on a glass slide and were allowed to from gel at RT. The glass slides were placed in a vacuum desiccator and dried under vacuum for nearly 6 h to obtain the xerogels. PXRD data of each sample was collected using Bruker D8 Advance diffractometer with CuKα source (1.5406 Å). Diffraction data were collected at 2θ angle from 1° to 30° using a 0.01° step size and 0.5 s per step. Low angle diffraction data was collected by keeping the motorized divergence slit in automatic mode so as to maintain the X-ray beam footprint on the sample to12 x 12 mm. Further, the position sensitive detector (Lynxeye) channels were reduced to minimize the background X-ray scattering entering the detector.

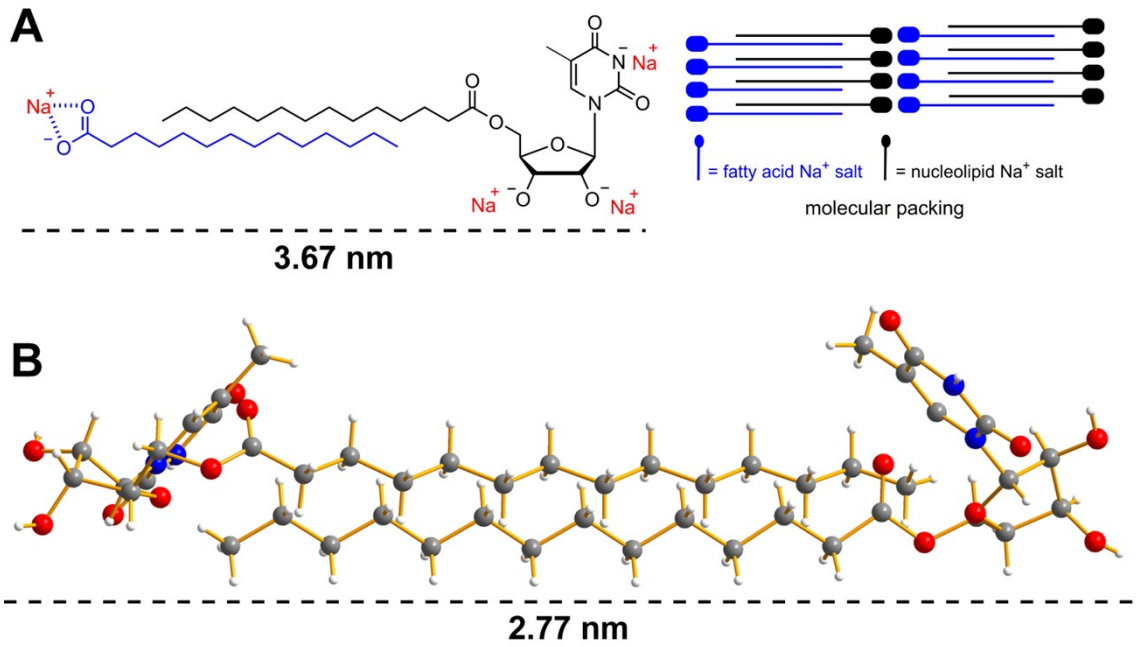

Fig. S14 (**A**) PXRD data of hydrogel of **3b** gave an interlayer distance of 3.67 nm and indicated the formation of a lamellar arrangement due to interdigitation. Based on PXRD and NMR experiments, we propose a model for the formation of heterotypic hydrogel network. Partial hydrolysis of **3b** results in the formation of myristate, which interdigitates with rest of the nucleolipid and then interacts in a head to head and tail to tail fashion forming a lamellar assembly.
(**B**) X-ray crystal structure of fully interdigitated structure of **3b** as viewed using Diamond 3.0. Atoms are coded as follows: off white, hydrogen; dark gray, carbon; blue, nitrogen; red, oxygen.

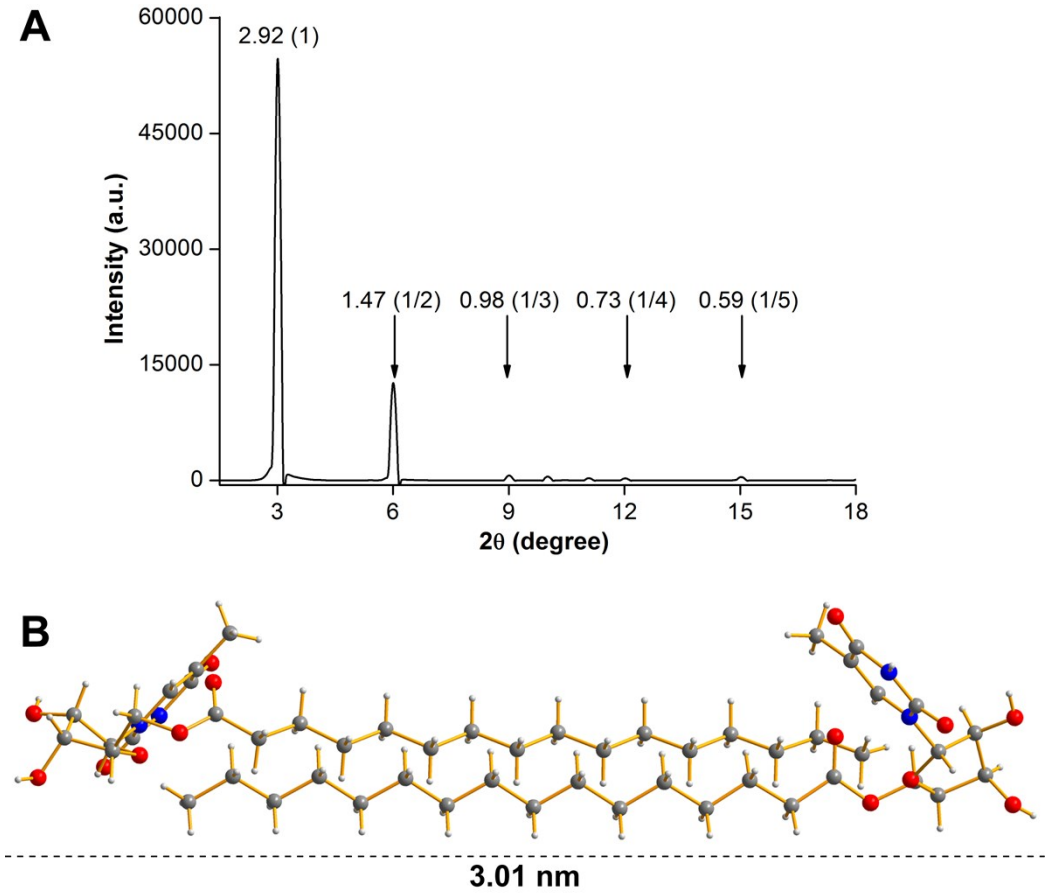

Fig. S15 PXRD spectrum of xerogel of **3c** organogel in benzene. Layer spacing (nm) for prominent diffraction peaks and their relative ratios are given in bracket.
(**B**) X-ray crystal structure of fully interdigitated structure of **3c** as viewed using Diamond 3.0. Atoms are coded as follows: off white, hydrogen; dark gray, carbon; blue, nitrogen; red, oxygen.

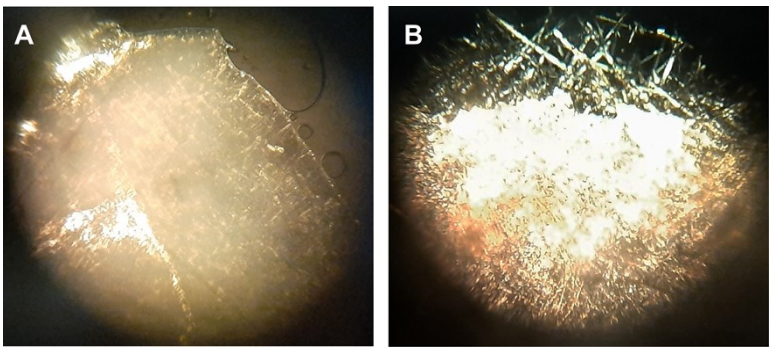

Fig. S16 Polarized light microscope images of **3b** hydrogel formed in the presence of NaOH (A) and organogel formed in chloroform (B).

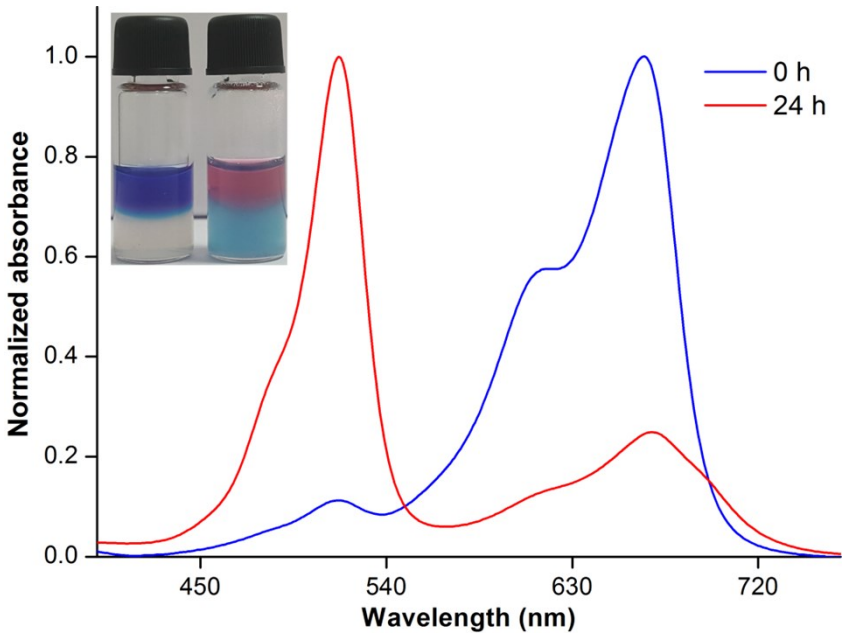

Fig. S17 Absorption spectra of the supernatant containing an equimolar mixture of dyes (MB and EY) incubated on the surface of **3b** hydrogel at 0 h and 24 h. Concentration of the dye mixture was 0.25 mM. Inset: picture of the vial at 0 h and 24 h.

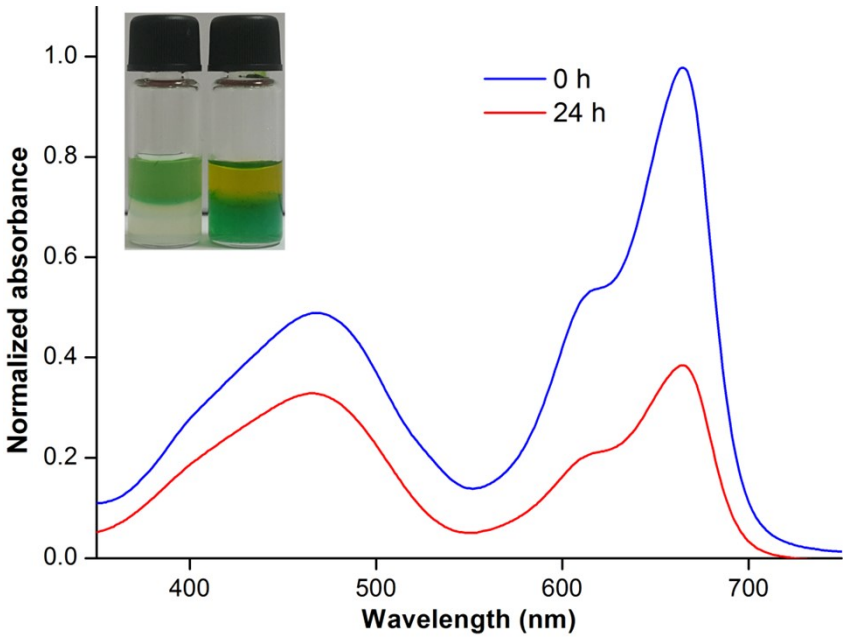

Fig. S18 Absorption spectra of the supernatant containing an equimolar mixture of dyes (MB and MO) incubated on the surface of **3b** hydrogel at 0 h and 24 h. Concentration of the dye mixture was 0.25 mM. Inset: picture of the vial at 0 h and 24 h.

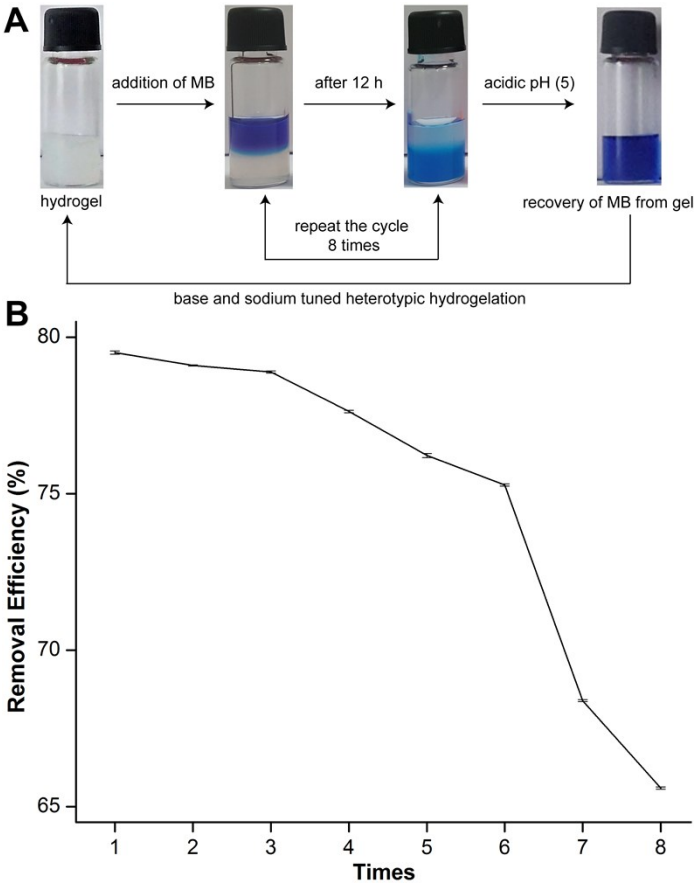

Fig. S19 (A) Picture showing the steps involved in the investigation of the recyclability of **3b** hydrogel in adsorbing dyes (e.g., MB). (**B**) Removal efficiency determined using absorbance of supernatant is plotted against number of cycles. See experimental section for details.

5. NMR spectra

^{1}H NMR of nucleolipid **3a** in DMSO-d_6

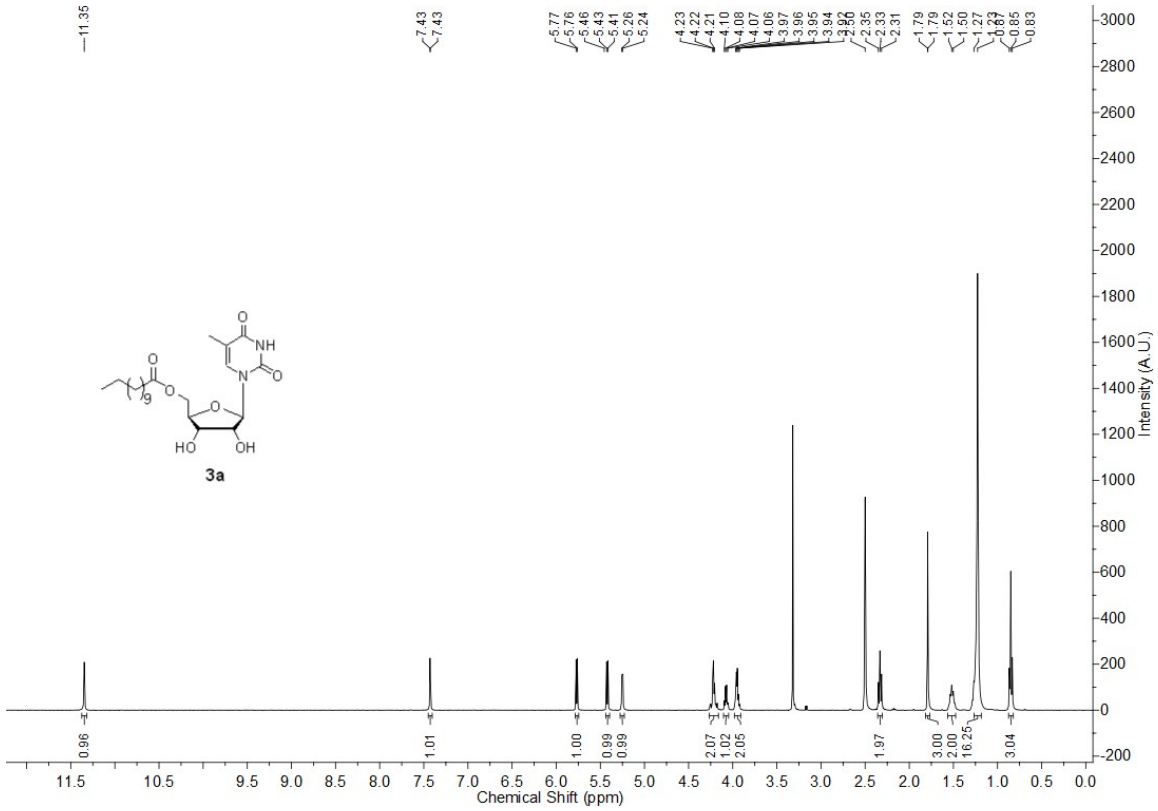

^{13}C NMR of nucleolipid **3a** in DMSO-d_6

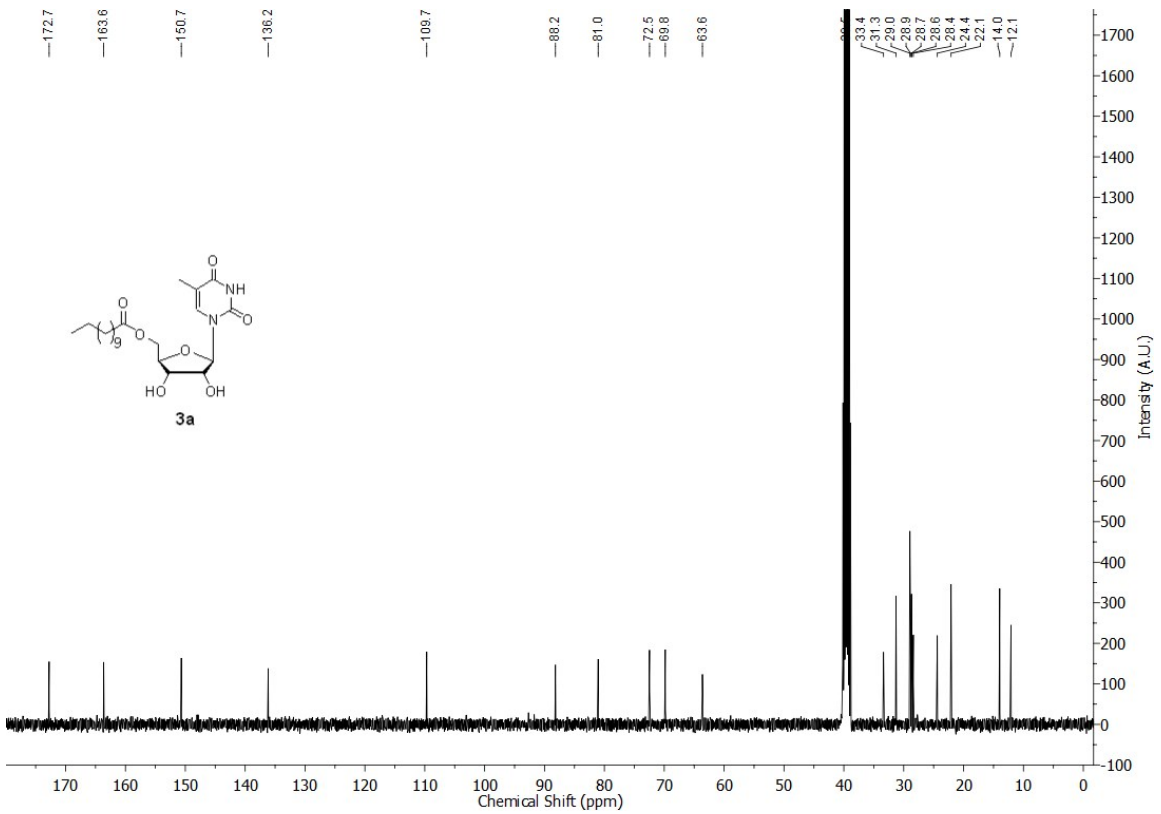

^{1}H NMR of nucleolipid **3b** in DMSO-d_6

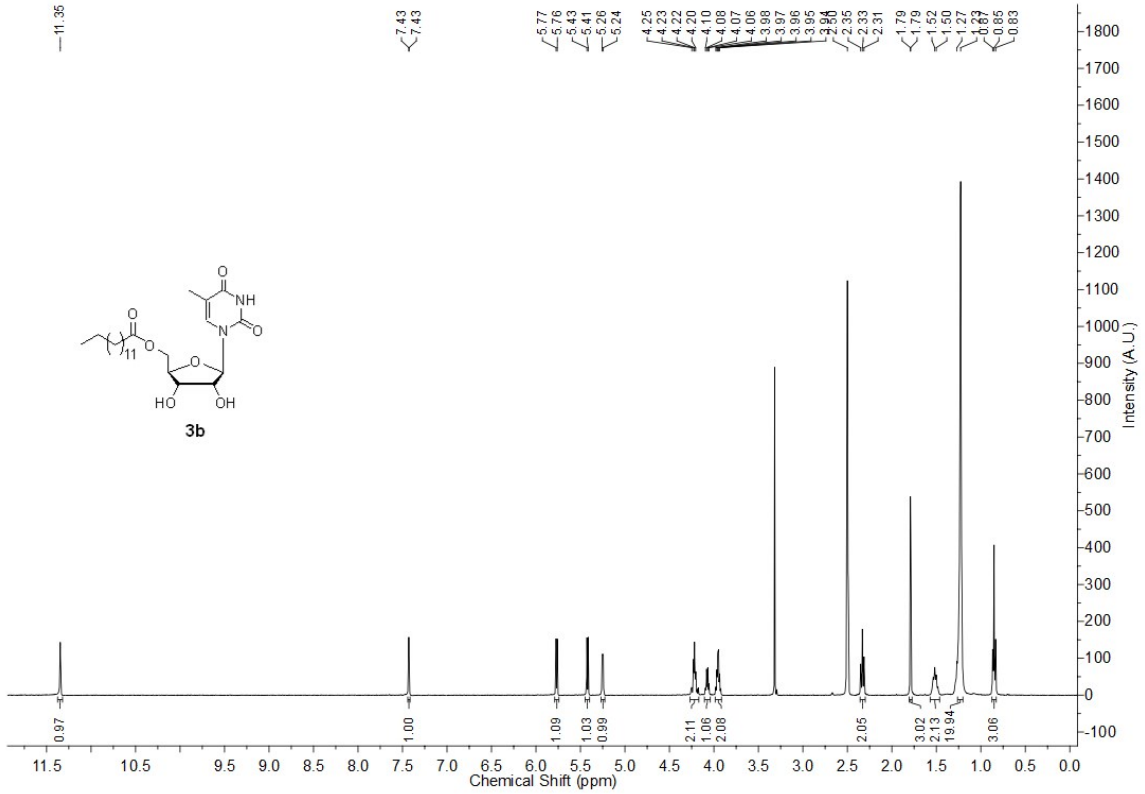

^{13}C NMR of nucleolipid **3b** in DMSO-d_6

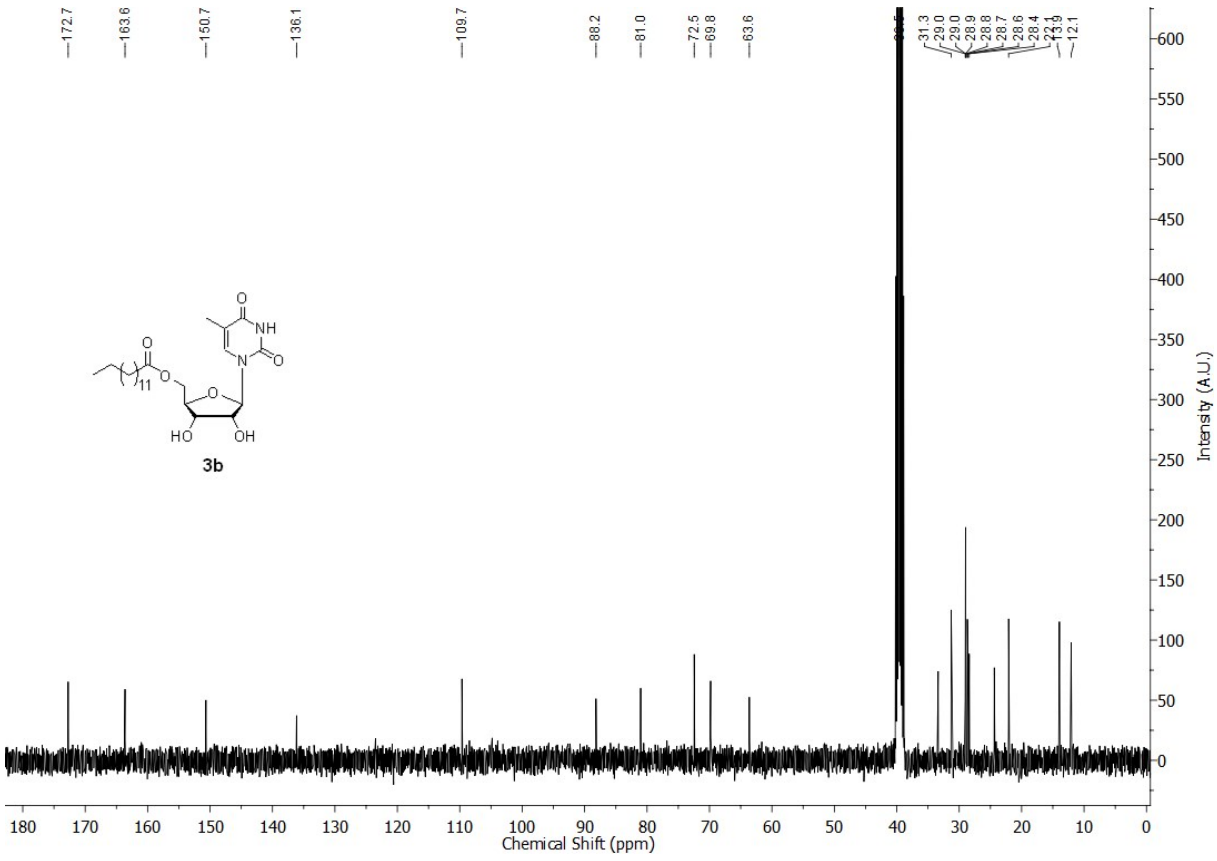

^{1}H NMR of nucleolipid **3c** in DMSO-d_6

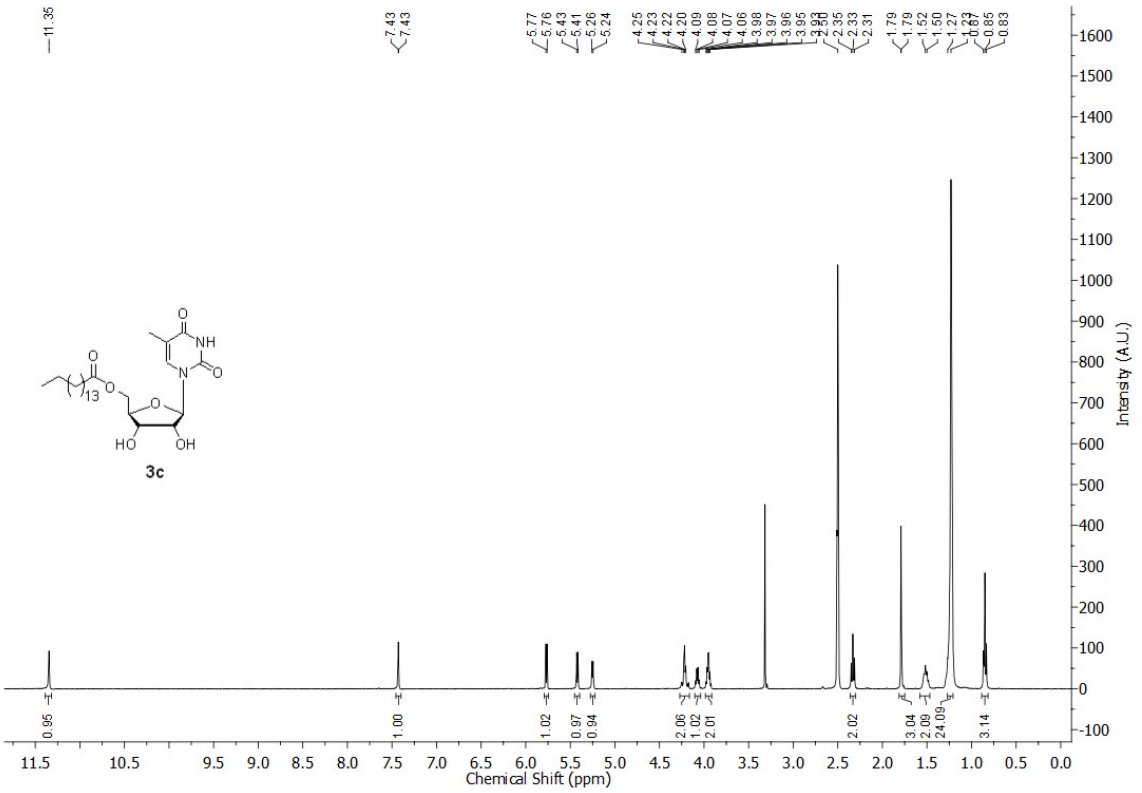

^{13}CNMR of nucleolipid **3c** in DMSO-d_6

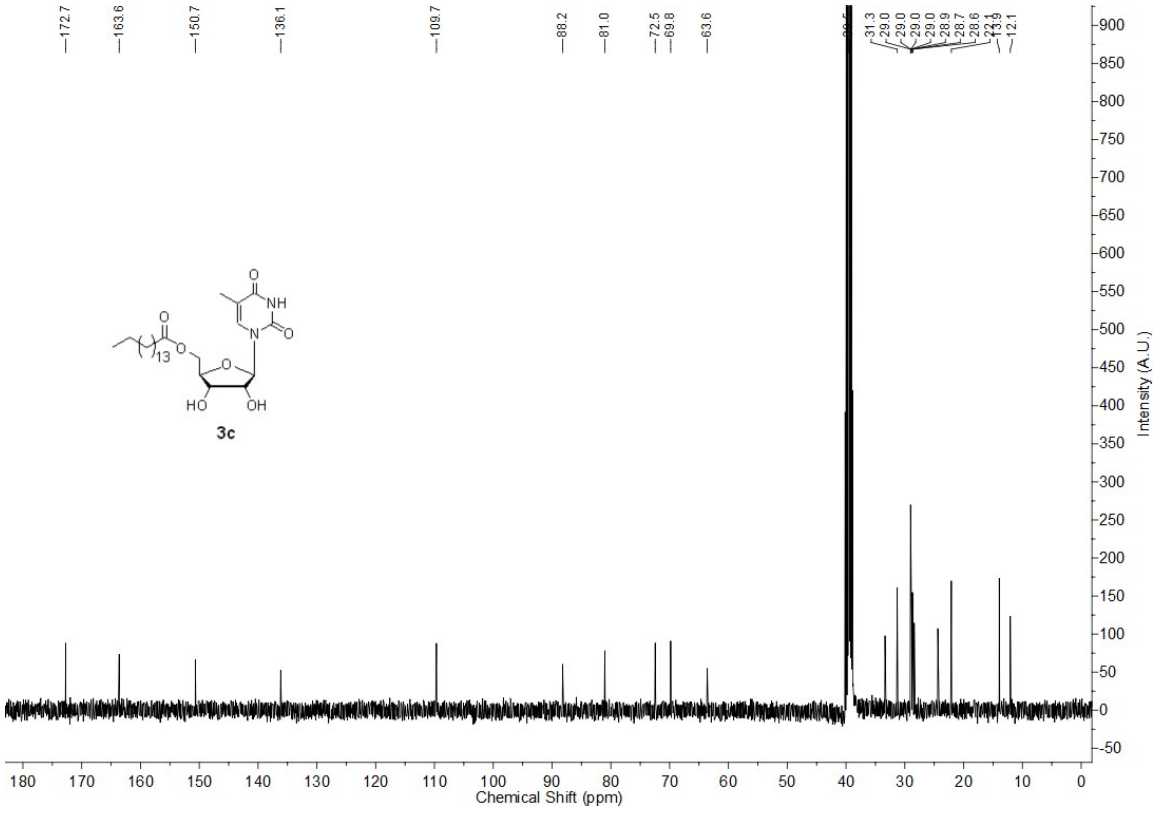

^{1}H NMR of nucleolipid **4a** in DMSO-d_6

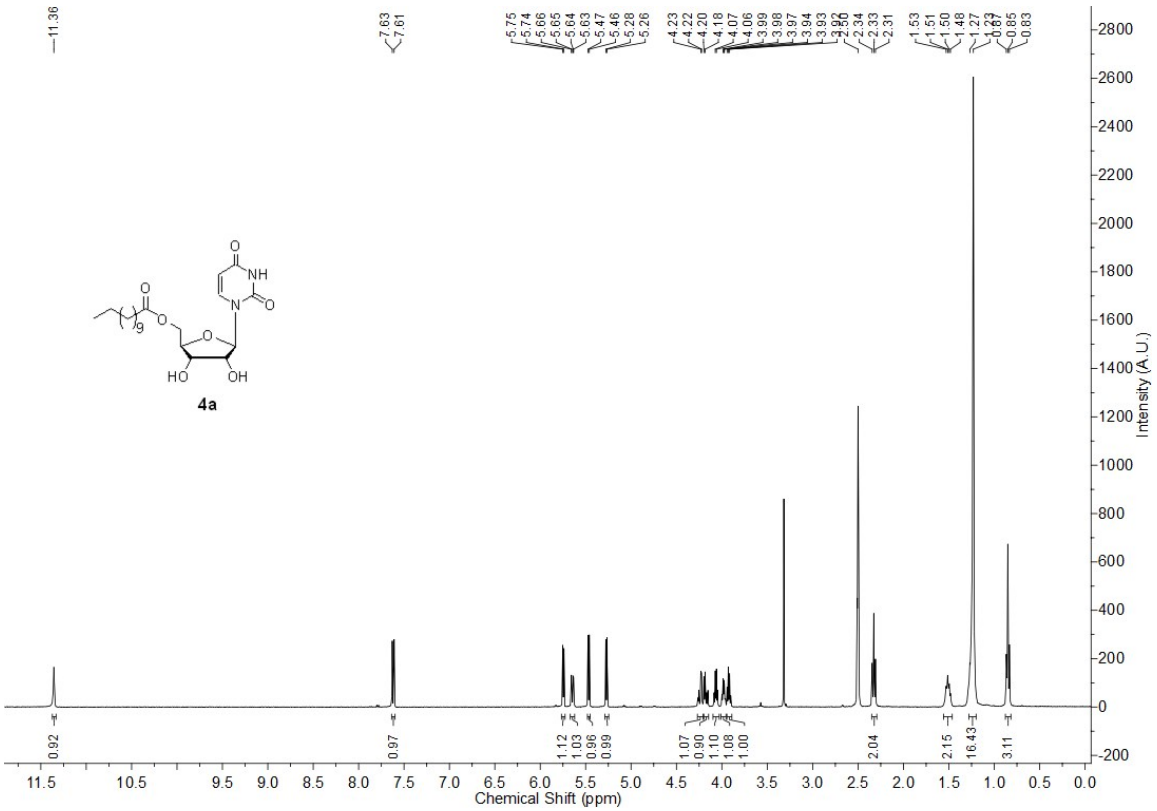

^{13}C NMR of nucleolipid **4a** in DMSO-d_6

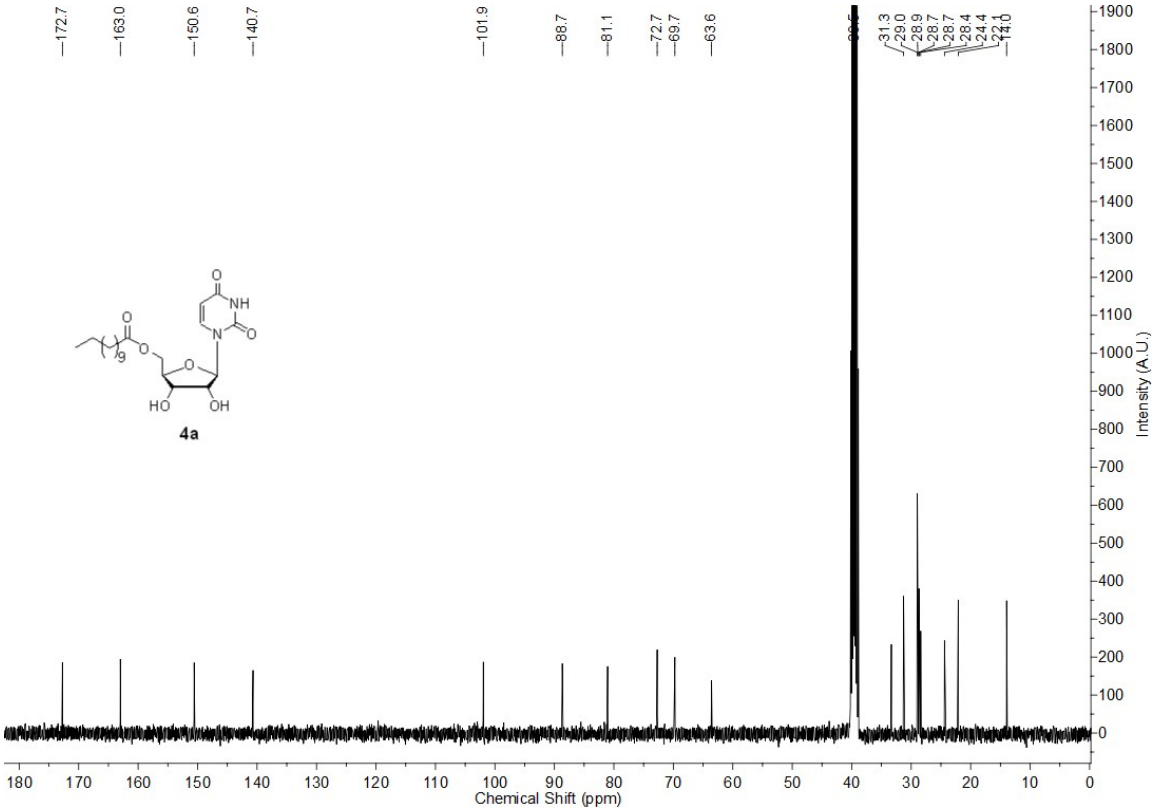

^{1}H NMR of nucleolipid **4b** in DMSO-d_6

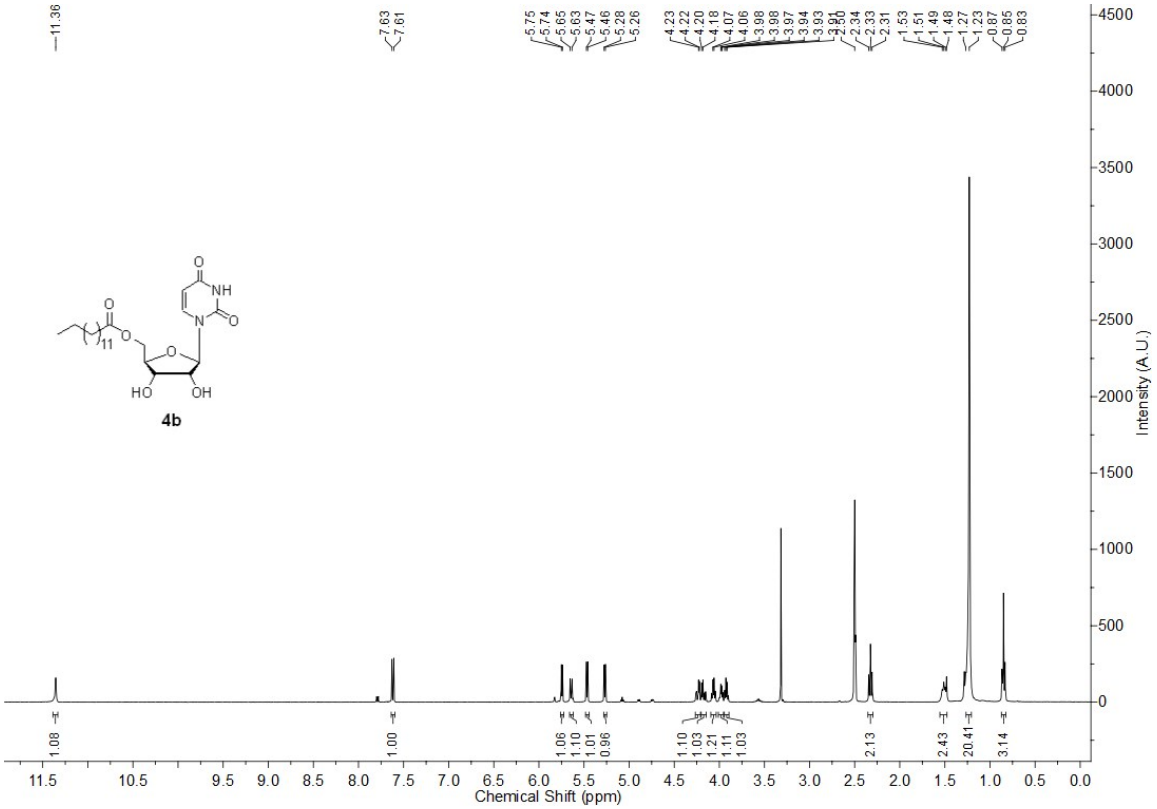

^{13}C NMR of nucleolipid **4b** in DMSO-d_6

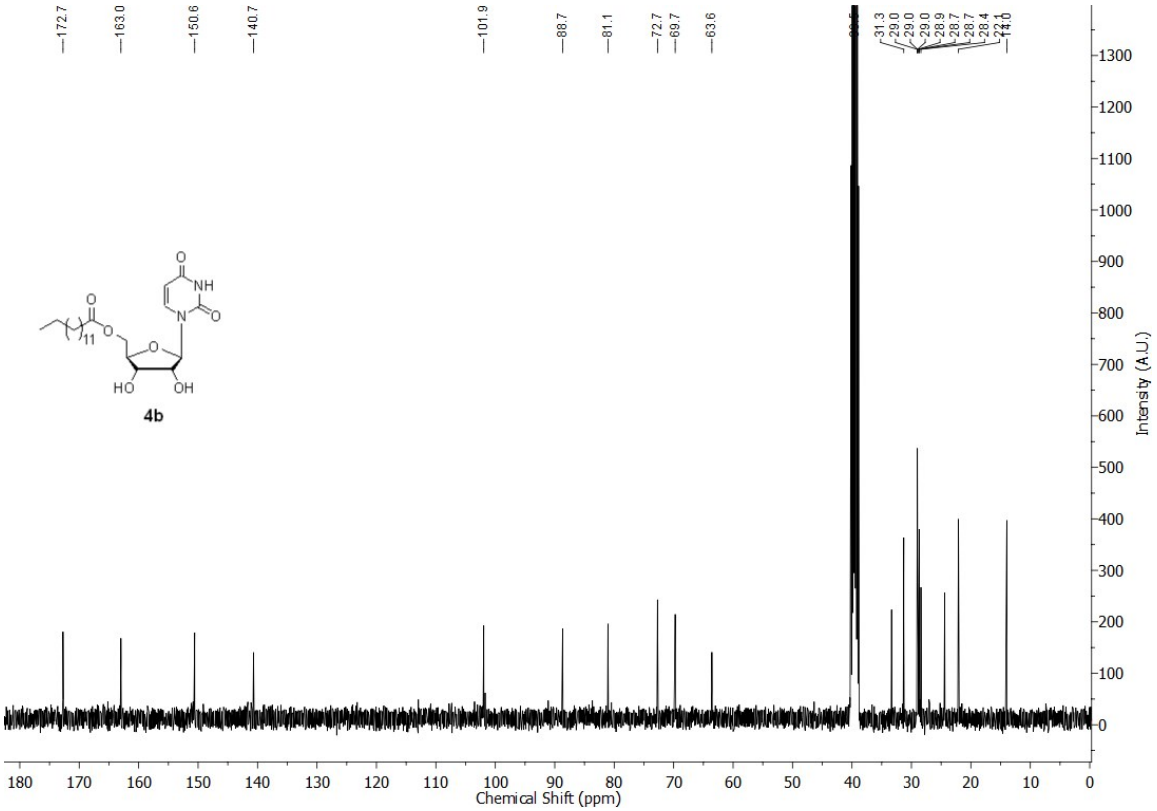

^{1}H NMR of nucleolipid **4c** in DMSO-d_6

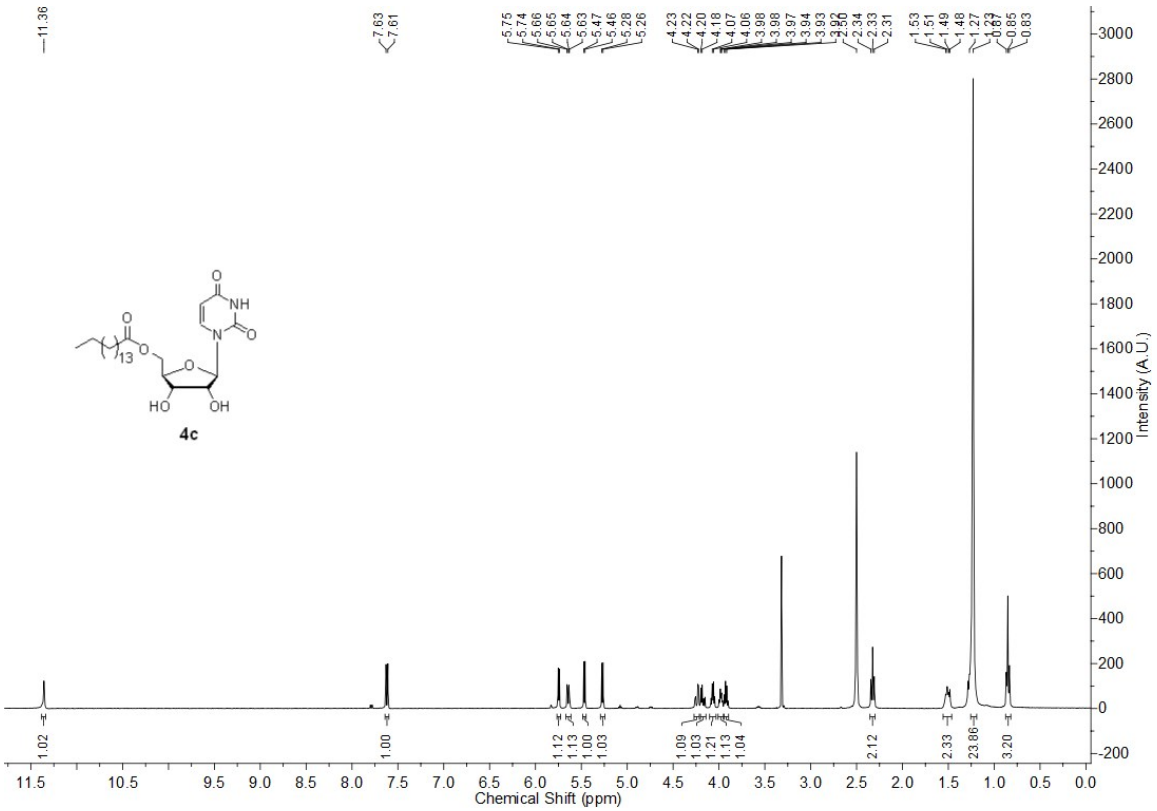

^{13}C NMR of nucleolipid **4c** in DMSO-d_6